Chapter 11
Biocontrol of Diamondback Moth, *Plutella xylostella*, with *Beauveria bassiana* and Its Metabolites

Liande Wang, Minsheng You, and Haichuan Wang

11.1 Introduction

The development of resistance to chemical insecticides and concerns over the deleterious effects of chemicals on environmental and human safety have provided a strong impetus for the development of microbial control agents for use in integrated control of insect pests. A diverse assemblage of microorganisms are currently under consideration as control agents of insects, including viruses, bacteria, protozoans, and fungi. Fungi will not be cure-alls for pest problems on all crops and in all agricultural settings, and it is unlikely that they will ever totally supplant the management of insect pests with chemical insecticides. Nevertheless, they represent a valuable management resource to be utilized within an IPM framework and will contribute significantly to reductions in chemical pesticide use (Lacey and Goettel 1995). However, the research development and final commercialization of fungal biological control agents (BCAs) continue to confront a number of obstacles, ranging from elucidating important basic biological knowledge to socioeconomic factors (Butt et al. 2001). Currently, considerable advances have been made in the infection mechanism (Wang et al. 2007, 2010). In this chapter, we present the biocontrol of diamondback moth (DBM), *Plutella xylostella* with *Beauveria bassiana* and its metabolites, with an elucidation on the infection behavior of *B. bassiana* to *P. xylostella* and virulence of the fungal isolate and its metabolites. The fungi that have received the majority of attention for *P. xylostella* control are the Deuteromycetes because of their prevalence, possibility for production on artificial media, ease of application, and relatively long shelf lives.

L. Wang (✉) • M. You
Institute of Applied Ecology, Key Laboratory of Biopesticide and Chemical Biology, MOE, Fujian Agriculture and Forestry University, Fuzhou 350002, China
e-mail: wang_liande@126.com

H. Wang
University of Nebraska-Lincoln, 312 Entomology Hall, Lincoln, NE 68583, USA

K.S. Sree, A. Varma (eds.), *Biocontrol of Lepidopteran Pests*, Soil Biology 43,
DOI 10.1007/978-3-319-14499-3_11

11.2 Virulence of Different *B. bassiana* Strains to *P. xylostella*

Wang (1999) bioassayed four strains of *B. bassiana* (Bb-100, Bb-71, Bb62, and Bb-38, conidial spore suspension 3×10^7 conidia/ml) to *P. xylostella* (second and third instars) in both laboratory and a small-scale field (in the campus of Fujian Agriculture and Forestry University, Fuzhou, PR China). As observed in Figs. 11.1 and 11.2, larvae became infected as they were inoculated. A time-mortality relationship was seen to exist. In the field and laboratory experiments, Bb-100 showed the strongest ability to kill the insect host. Due to imprecise mortality estimates in the field, it was difficult to quantify the effect of LT_{50}. The LT_{50} to DBM with

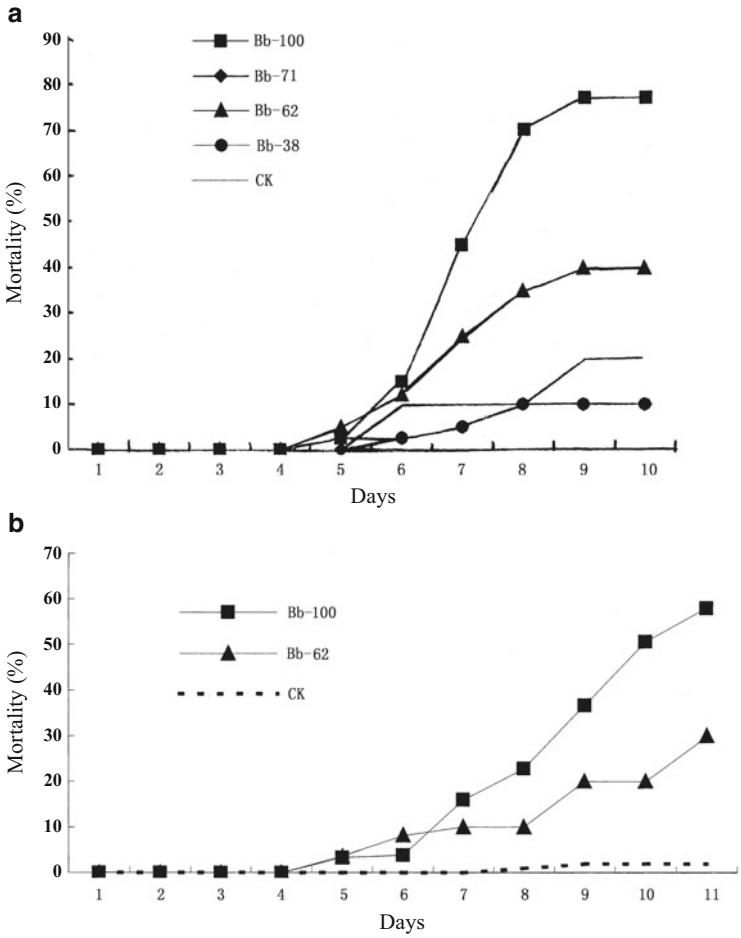

Fig. 11.1 Virulence assay of four strains of *B. bassiana* against *P. xylostella* in (**a**) laboratory, (**b**) field (cf. Wang 1999; You et al. 2004)

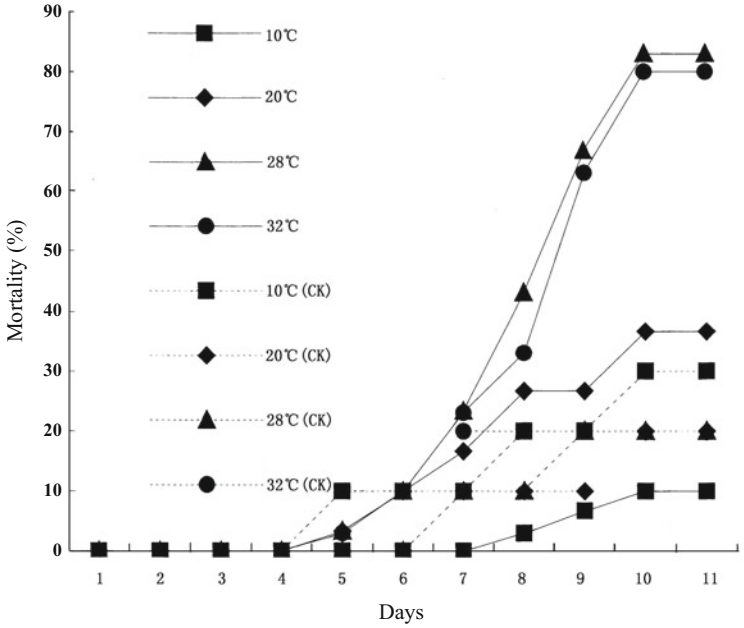

Fig. 11.2 Virulence assay of strain Bb-100 of *B. bassiana* against *P. xylostella* at different temperatures (cf. Wang 1999; You et al. 2004)

Bb-100 was 8.5 days in the laboratory; the starting time was over 5 days in the laboratory and field. Among the four strains, Bb-38 exhibited the least virulence to DBM.

To reveal environmental effect on the virulence of *B. bassiana*, a simple matrix treatment considering *P. xylostella* and Bb-100 was carried out in the laboratory. The infectious ability of Bb-100 strongly varied with temperature. Figure 11.2 indicates that the mortality approximately began 4–5 days after application. The highest level of mortality was seen at 28 °C, but the fastest time to knock down the host was at 32 °C. Low temperature delayed the activity in infection. On the other hand, it was reported that relative humidity could influence the mortality of *P. xylostella* (Masuda 1998). Undoubtedly, temperature is one of the basic factors of virulence of *B. bassiana*.

11.3 Infection Behavior of *B. bassiana* to *P. xylostella*

11.3.1 Infection Process

The process of fungal infection involves four steps: adhesion, germination, differentiation, and penetration (St. Leger et al. 1996).

11.3.1.1 Attachment

Attachment of fungal spores to the host is a prerequisite for further parasitic events and takes place together with host recognition. Conidial attachment is one of the dominant steps in the course of infection of entomopathogenic fungi. This experiment focused on the initial behavior of the conidia of *B. bassiana* on the cuticle of the third instar of *P. xylostella*. With the infection process used, conidia were commonly found on the ventral side, in segmental vicinity, and on no-sticklike area on the host. Clearly, the conidia (1.8–2.8 μm) are almost as large as the size of space among hairs on the cuticle surface of *P. xylostella*; therefore, conidia were getting a full touch with *P. xylostella* cuticle. Despite this, there were still some conidia which contacted larval epicuticle at rare hairy region (e.g., intertegumental membrane, abdomen, etc.), germinated, and breached the epicuticle (Figs. 11.3 and 11.4). The increasing evidence of conidial germination was clearly presented after 24 h. The surface of conidia possesses an outer layer of interwoven pins (Figs. 11.5 and 11.6). The structure is unique to the conidial stage, not detected on the vegetative cells (hyphal body, mycelium). The interwoven pins were arranged in groups, mainly in a vertical position, but near the top, there were several pins positioned horizontally (Fig. 11.6, arrows; Wang 1999).

This structure was rarely observed, only in conidia submerged in liquid media, and not those on dry. The superficial structure on a conidium was as similar as indicated in Fig. 11.6. The existence of such structures suggests that the topography of the conidium assists the recognition or attachment between conidium and host (Zhai and Huang 1995; Bidochka et al. 1993). After coming in contact with the cuticle of both hosts, conidium began to release some mucilage materials around the conidium (Fig. 11.7a). Obviously, at the contact point or nearby, materials cover the outer layer of conidia, which may serve as glue (Large et al. 1988). Compared with other parts of the conidium, the mucus around the part touching the cuticle was thicker. After germination, mucilage covered the outer conidium wall, but at the top

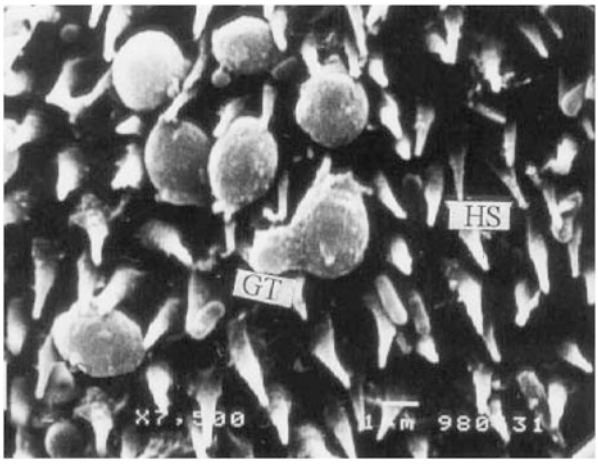

Fig. 11.3 Superficial epicuticle of *P. xylostella* infected by Bb-100 under SEM, conidia (C), germ tube (GT), hairs (HS) (cf. Wang 1999; You et al. 2004)

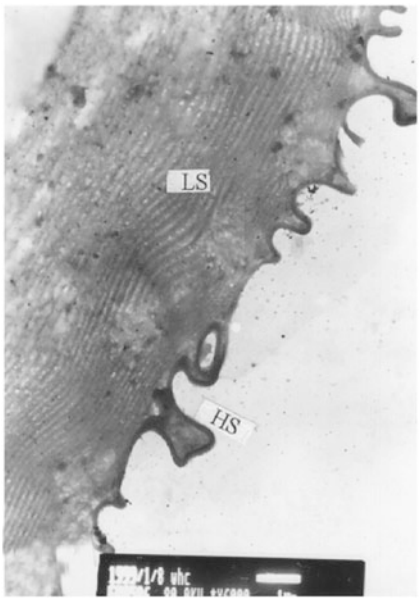

Fig. 11.4 Cross section of the cuticle of *P. xylostella* under SEM, hairs (HS) (cf. Wang 1999; You et al. 2004)

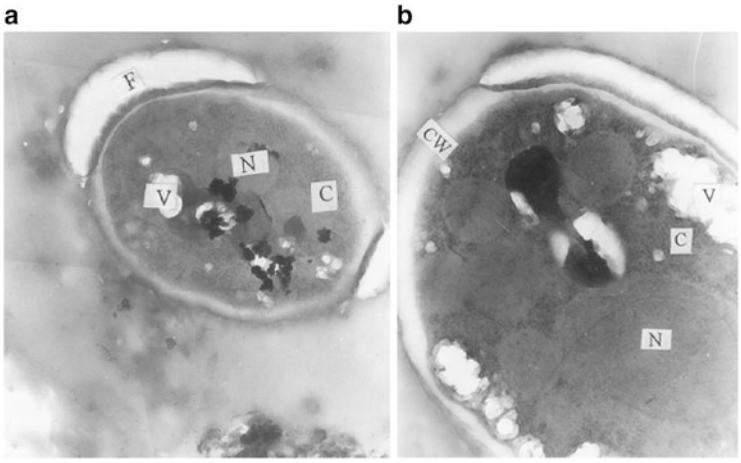

Fig. 11.5 TEM of a conidium, conidium (C), conidial wall (CW), vacuole (V), nucleus (N), floccule (F) (cf. Wang 1999; You et al. 2004)

of the germ tube, the mucilage was much thicker than other parts (Fig. 11.7b, c under TEM). At this stage, no septum was observed between the germ tube and maternal conidium. Underneath, comparing with the parts nearby, the cuticle of *P. xylostella* was turned to gray in color, showing a distinct deformation of the epicuticle. It is suggested that within either part of the germ tube or contacting part of the conidium with the cuticle would be the most metabolically active section; the

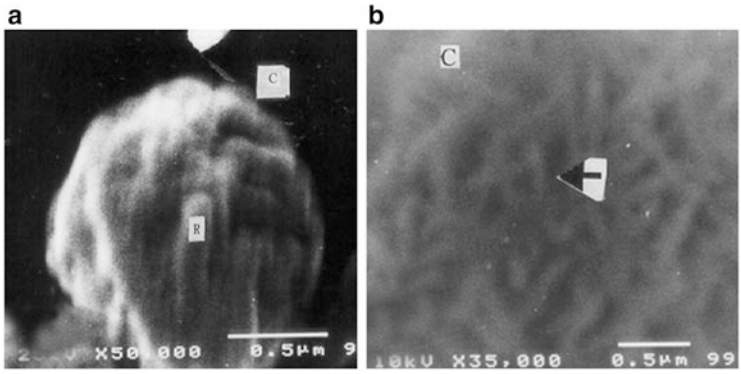

Fig. 11.6 (**a**) A view of the conidium under TEM, conidium (C), rodlet (R); (**b**) a general view of the conidium under TEM, conidium (C), rodlet-like structure (*arrow*) (cf. Wang 1999; You et al. 2004)

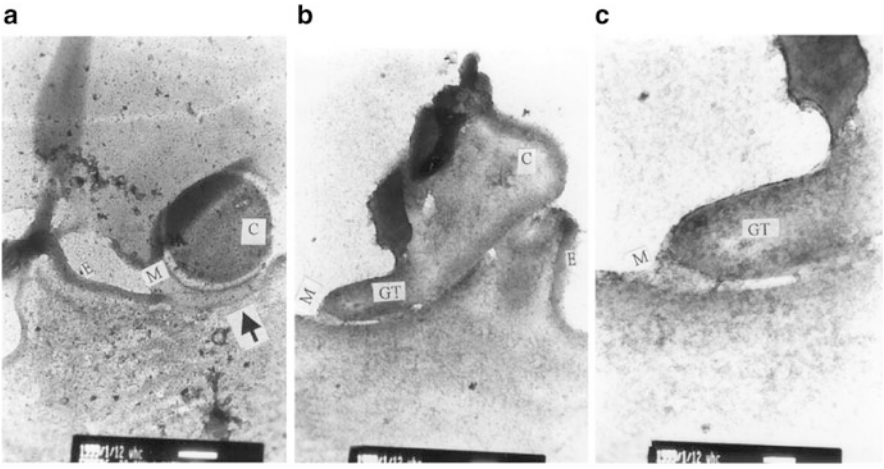

Fig. 11.7 Conidium on the cuticle of *P. xylostella* under TEM, conidium or conidia (C), mucilage (M), epicuticle (E), germ tube (GT); (**a**) conidium falling down on cuticle of *P. xylostella*, arrow indicating degraded epicuticle, bar = 500 nm; (**b** and **c**) germinating conidia on the epicuticle of *P. xylostella*, bar = 100 nm (cf. Wang 1999; You et al. 2004)

mucilage outside was secreted by the conidium and germ tube themselves (Wang 1999).

11.3.1.2 Germination

The germination tests proceeded after inoculation on different hosts in the laboratory (Table 11.1). Even within a given laboratory, the germination ratio varied with

Table 11.1 Assay of conidial germination and appressorial formation on different media

Strain	Item	Rate (%)/+0.0125 YEM			Rate (%)/+sterilized water		
		12 h	24 h	36 h	12 h	24 h	36 h
Bb-100	GC	3.5	18	25	2.0	6.6	20
	AP	1.2	3.0	5.0	1.0	2.1	3.0
Bb-62	GC	2.2	5.6	5.6	1.0	3.8	6
	AP	0.5	1.7	1.7	0.1	1.6	1.6
Bb-71	GC	1.0	4.0	5.2	0.0	4.0	4.1
	AP	0.0	1.8	2.7	0.0	2.0	2.5
Bb-38	GC	1.5	26	30	1.0	25	30
	AP	0.4	11	19	0.0	14	19

Suspension 3×10^7 conidia/ml + 0.0125 YEM, 28 °C pH = 6.5 or suspension 3×10^7 conidia/ml + sterilized water, 28 °C pH = 6.5, germinating conidia (GC), appressoria (AP), cf. Wang (1999) and You et al. (2004)

the strain and host. Clearly, the conidia could germinate on all hosts, after 24 h. With the elongation of the incubation time, the number of germinated conidia (GC) on all hosts increased linearly. In treatments adding 1.25 % YEM, the germination ratio was higher than those with only sterilized water. The result that suitable addition of nutrient could stimulate the germination of conidia was consistent with Fan and Li (1994) and St. Leger et al. (1991, 1989). Bb-38 could easily germinate on *P. xylostella* (Wang 1999).

Under the conditions of 28 °C, pH = 6, 80 % RH, in the four strains of *B. bassiana*, the amount of conidial germination increased with time. With the infection process used, the GC could be found at any part of the cuticle including the head, thorax, and elytra under SEM (Fig. 11.8).

On cuticle, although some conidia only contacted with horn-like nodules, they still appeared in taxis bending toward the cuticle (Fig. 11.8, under SEM). The germ tube of Bb-100 on the abdomen of *P. xylostella* (Fig. 11.8V) had less orientation, but on the head and other parts (Figs. 11.7 and 11.8I, II), Bb-71 showed a little taxis (Fig. 11.8III, IV). Taking the materials that exist on the epicuticle into consideration, differences in conidial orientation are probably due to components that can have prohibiting or stimulating functions on conidia (Zhai and Huang 1997; St. Leger et al. 1994). Before penetrating into *P. xylostella*, the germ tubes were 2.2–6.6 μm in length in Bb-100 and Bb-62. In Bb-71, germ tube length was around 11.2 μm. Extensive amounts of errant-growing hyphae were rare to see, but limited amounts of errant growth followed by eventual penetration over the surface were seen (Fig. 11.8VI, VII for strain Bb-100 on *P. xylostella*). At early stage about 24 h, few big vacuoles filled the whole conidium; the bud of the germ tube formed at random, into which the vacuole expanded (Fig. 11.8VIII for strain Bb-100). After 48 h, nuclear division was finished, materials in the conidium were transmitted toward the germ tube, a big vacuole was formed consequently, and the top of germ tubes sometimes tended to be thin (Fig. 11.8IX for strain Bb-100). In late stages, the septum was formed between the conidium and germ tube, and daughter nuclei moved into the germ tube (Fig. 11.8X) (Wang 1999).

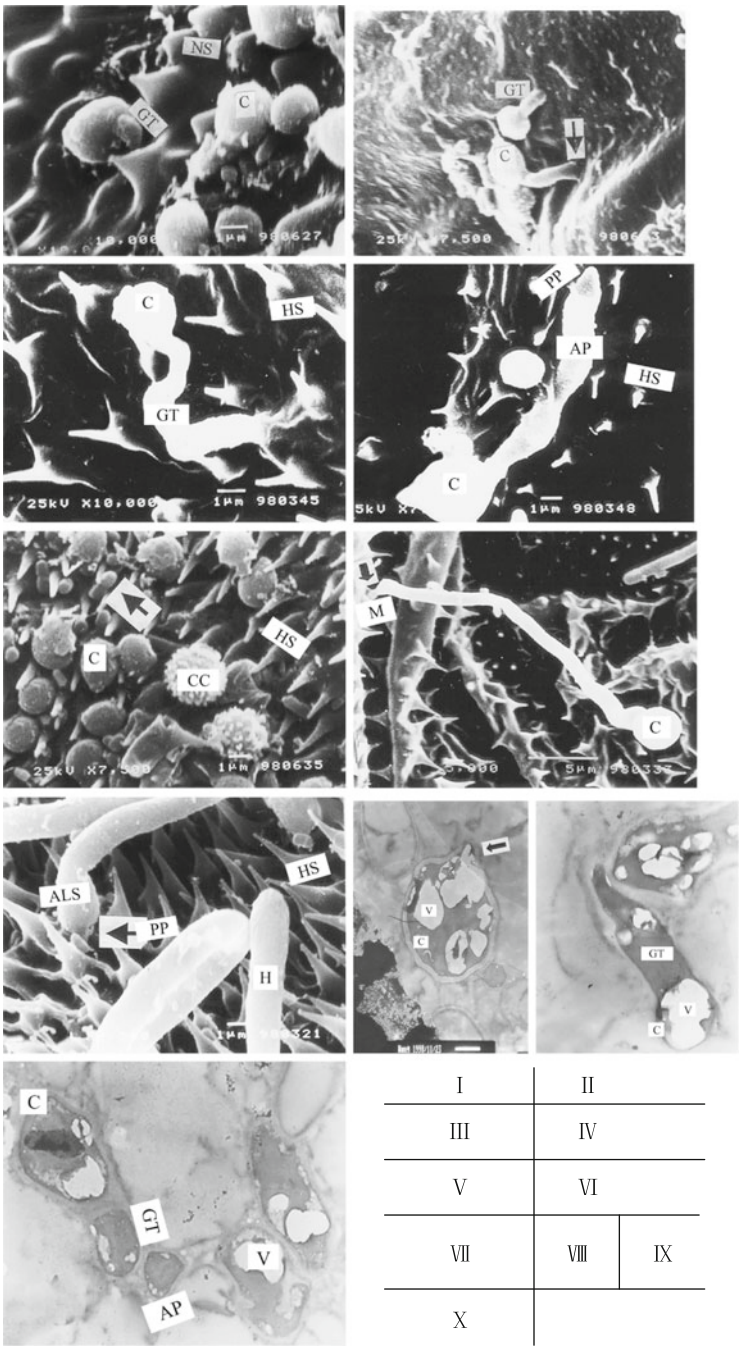

Fig. 11.8 (*I*) Superficial view of the thorax of *P. xylostella* infected with Bb-100 after 24 h under SEM, scale bar = 1 μm; (*II*) fine structure of the head of *P. xylostella* contaminated with Bb-100 after 24 h under SEM, germinating conidia (*arrow*), scale bar = 1 μm; (*III*) abdomen of *P. xylostella* contaminated by Bb-71 after over 36 h under SEM, hyphae penetrating into epicuticle

11.3.1.3 Appressoria

The second instar of *P. xylostella* was contaminated by four strains and provided a rich form of appressoria and appressoria-like structures. In Figs. 11.8IV, VII and 11.9I, II, a penetration peg for host penetration was produced, but the penetration peg was formed at a position near to germ tube in Fig. 11.9II, while it came into being at the tip of germ tube as in Figs. 11.8VII and 11.9I, II. Nearly all penetration pegs breached the cuticle. Enzyme activity was presented at the tip of the penetration peg as in Fig. 11.9II. Appressoria of *B. bassiana* were usually formed at the end of a germ tube of variable lengths and often terminated in a bulb from which a narrow hypha (penetration peg) emerged. Appressoria were occasionally formed apically on short germ tubes or directly from conidia (Fig. 11.9I, II). Evidence showed that no penetration peg or appressoria could still penetrate into the cuticle (Fig. 11.9III with Bb-71). Meanwhile, other appressoria-like structures were found (Fig. 11.8VI with Bb-100, Fig. 11.9IV with Bb-38); at the top of the germ tube, a penetration peg-like structure was produced (Wang 1999).

Under TEM, photographs of the internal structures of appressoria or appressoria-like structure were taken (Fig. 11.10I–III, appressoria-like structure, IV–IX appressoria). TEM photos presented that the pre-GT stood out, to which materials were moved from conidium (Fig. 11.10IV). There was a short stage of vigorous nuclear activity where the daughter nucleus spread inside a second time frame (Fig. 11.10V). The formation of septum was followed by the migration of the nuclei into the appressoria (Fig. 11.10IX). Inside the appressoria-like structure (Fig. 11.10I–III), conidial materials were transmitted from the conidia to the top part. The most frequent and biggest vacuoles could be found within the conidium and along the germ tube. Inside, nuclear division had been finished, and daughter nuclei could be seen in the germ tube. In late stage about 48 h, inside nuclei division had been finished; one daughter nuclei still remained in the conidium, while another moved through the germ tube and entered the forming appressorium. A septum usually was formed across the end of the germ tube, beginning to separate germ tube (appressoria) from conidia (Fig. 11.10IX). Beforehand, karyon division was

Fig. 11.8 (continued) (*arrow*), scale bar = 1 μm; (*IV*) superficial view of the abdomen of *P. xylostella* with Bb-71 after over 36 h under SEM, hyphae penetrating into the epicuticle (*arrow*), scale bar = 1 μm; (*V*) superficial view of the abdomen of *P. xylostella* infected with Bb-100 under SEM, conidia (*arrow*), scale bar = 1 μm; (*VI*) appressoria-like structure in Bb-100 ready to invade the epicuticle of *P. xylostella* after over 36 h under SEM, invading appressoria-like structure (*arrow*), scale bar = 1 μm; (*VII*) appressoria (Bb-38) penetrating the epicuticle of *P. xylostella* after over 36 h under SEM, a terminal swollen invading appressorium (*arrow*), scale bar = 1 μm; (*VIII*) cross section of conidia under TEM, bud of the germ tube (*arrow*), scale bar = 1 μm; (*IX*) germinated conidia under TEM, scale bar = 1,500 nm; (*X*) thin section of appressorium under TEM, scale bar = 1 μm; conidium (C), germ tube (GT), nodule structure (NS), hairs (HS), appressorium (AP), penetration peg (PP), contaminated conidia (CC), vacuole (V), nuclei (N), mucilage (M), appressoria-like structure (ALS), hyphae (H) (cf. Wang 1999; You et al. 2004)

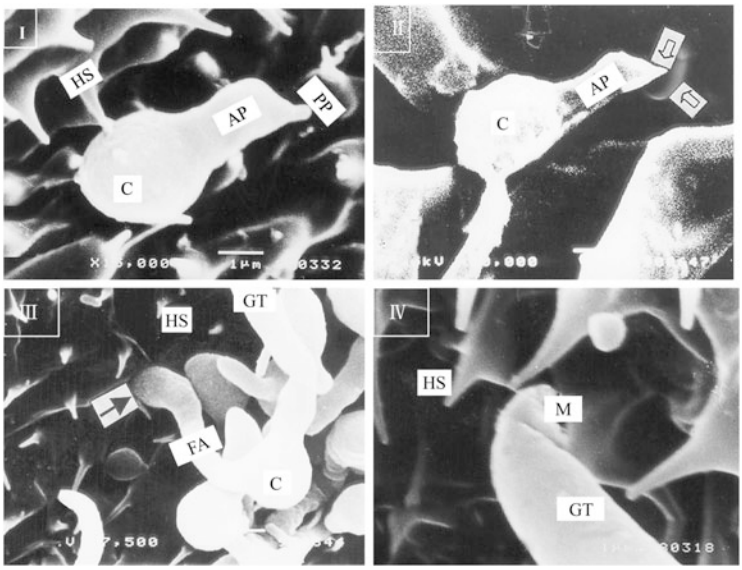

Fig. 11.9 Appressorium on the cuticle of *P. xylostella* contaminated by *B. bassiana* under SEM, conidia (C), germ tube (GT), hairs (HS), appressorium (AP), penetration peg (PP), fusiform appressorium (FA), mucilage (M); (*I*) and (*II*) contaminated by Bb-100; (*III*) contaminated by Bb-71, melanized tip of appressorium (*arrow*) during invasion; (*IV*) contaminated by Bb-38; scale bar = 1 μm (cf. Wang 1999; You et al. 2004)

processed prior to septum formation, but it is difficult to find. Clearly, the formation of septum symbolizes the finished and mature stage of appressoria. Sometimes mucus appeared at the top of appressoria (Fig. 11.10X–XII), but not in all. In Fig. 11.9III, the top of appressoria externally turned dark in color before penetration. Appressorial wall thickness was the same as conidia, but in some appressoria, a part of the top wall of appressorium was thickening (Fig. 11.10IX). Compared with appressoria, the germ tube wall was thinner than the conidia (Fig. 11.10X–XII). Inside, a great deal of vesicles could be found in maternal conidia, but in appressoria, vesicles were rare, especially at the top (Fig. 11.10IX, X) (Wang 1999).

11.3.1.4 Penetration

Penetration is another dominant step in the course of infection in entomopathogenic fungi. These experiments focused on the behavior of conidia of *B. bassiana* on the cuticle of the second instar of *P. xylostella*. The penetration was observed over 36 h contamination of host and could happen almost at any region with hole at the point of penetration of the cuticle, including the thorax (Fig. 11.8I), head (Fig. 11.8II), and abdomen (Fig. 11.8III–V). There were more penetrations at the rare hair region than regions with heavy hair. There was no errant growth of hyphae without

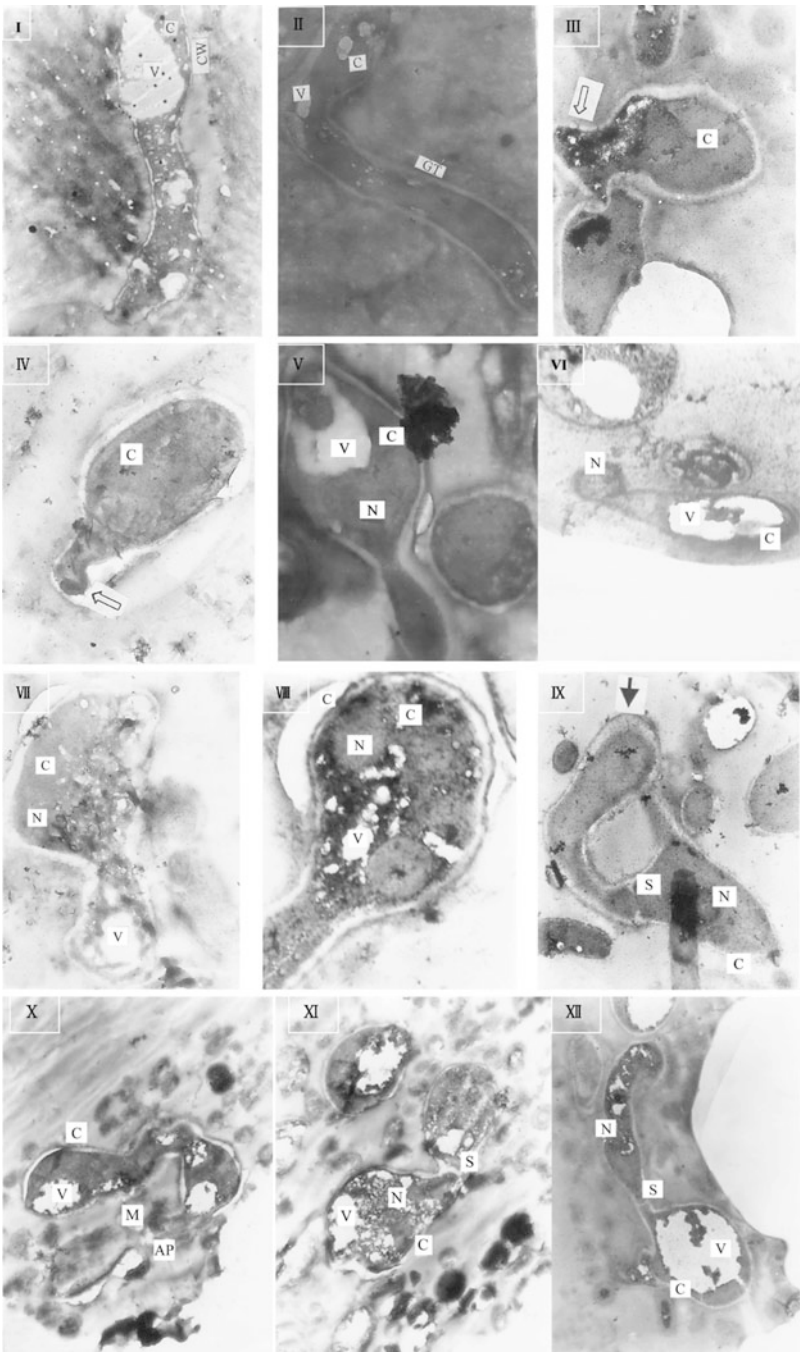

Fig. 11.10 Germ tube and appressoria under TEM (*I*) detailed germ tube, scale bar = 500 nm; (*II*) thin section of appressoria-like structure, scale bar = 500 nm; (*III*) appressoria-like structure, birdhead-like tip (*arrow*), scale bar = 500 nm; (*IV*) initial appressorial structure (*arrow*), scale bar = 200 nm; (*V*) early appressorial structure (*arrow*), scale bar = 1 μm; (*VI–VIII*) appressoria-

penetration observed. Penetration peg was formed at the tip or near the tip position of appressoria (Fig. 11.8III), which was succeeding in the cuticle. In both Bb-100 and Bb-62, most germ tubes were short and thin at the top part on *P. xylostella* when penetrating. It was also noted that terminal swelling on the end of the germ tube turned dark when breaking down the cuticle of *P. xylostella* (Fig. 11.9III with strain Bb-71). The invading hypha was quite simple, without any change at the top. No such phenomenon was found in three others (strain Ba-100, Ba-38, and Ba-62). A cross section of the cuticle of both *P. xylostella* (Fig. 11.10) was made to record the differences between them at the ultrastructural level. There is a lamellate structure under the epicuticle of the abdomen, seeing no nuance between them. Nevertheless, the gold-coloidal technique (gold-chitinase complexes) revealed some differences. Particles could be found in main parts of the cuticle in both pests. In early stages of penetration, mucilage was found at the edge of the top of the germ tube contacting with the cuticle of *P. xylostella* before breaching it (Fig. 11.7a); epicuticle deformation was also observed. A detailed micrography revealed that mucilage was double layer (Fig. 11.11I). Meanwhile, mucilage also appeared at no contacting part (at the edge of the top of the germ tube) (Fig. 11.11I–III). Under the conidium, there was a great reduction in thickness of the epicuticle of the host or even a complete absence of cuticle material (Fig. 11.11III). The deformation of epicuticle appeared under the conidium otherwise (Fig. 11.12I). These results suggest that (1) within the top part of germ tube (or appressoria) would be the most active site of enzyme metabolism and (2) results confirm the hypothesis that pathogen invasion is a combination of enzyme and mechanical pressure (Zhai and Huang 1995). On *P. xylostella*, birdhead-like appressoria were observed, but were rarely seen (Fig. 11.9I, II). Few appressoria were presented on *P. xylostella*, but their shape was the same as those generated by Bb-100. When breaching the cuticle of *P. xylostella*, mucus still covered at the top of the germ tube externally (Fig. 11.12I). After breaking down, materials inside the conidium migrated into the germ tube, which made the germ tube fully expand and the conidium was partly emptied. At the same time, daughter nuclei also moved into the germ tube (Fig. 11.12II) on *P. xylostella* with Bb-100; mucus sealed around cleavage could be found (Fig. 11.12III, IV). Without touching with any substance, mucilage could be secreted by appressoria (Fig. 11.10IX); meanwhile, septum was not found. It is proposed that mucilage material secreted by *B. bassiana* would assist fungi's infection. Near the germ tube, hyphal bodies were formed, which were full inside; nuclei were clearly seen without any vesicles (Fig. 11.12III). In later stages (after over 5–7 days on *P. xylostella*), hyphal bodies and blastospores fully filled the host body (Fig. 11.13I under TEM) and cuticle was destroyed (Fig. 11.13II under TEM).

Fig. 11.10 (continued) like structure, scale bar = 200 nm; (*IX*) appressoria in middle stage, scale bar = 1 μm; (*X–XII*) detailed appressorial structure, scale bar = 1 μm; conidia (C), conidia wall (CW), germ tube (GT), nodule structure (NS), hairs (HS), appressorium (AP), penetration peg (PP), contaminated conidia (CC), vacuole (V), nuclei (N), fusiform appressoria (FA), mucilage (M), septum (S) (cf. Wang 1999; You et al. 2004)

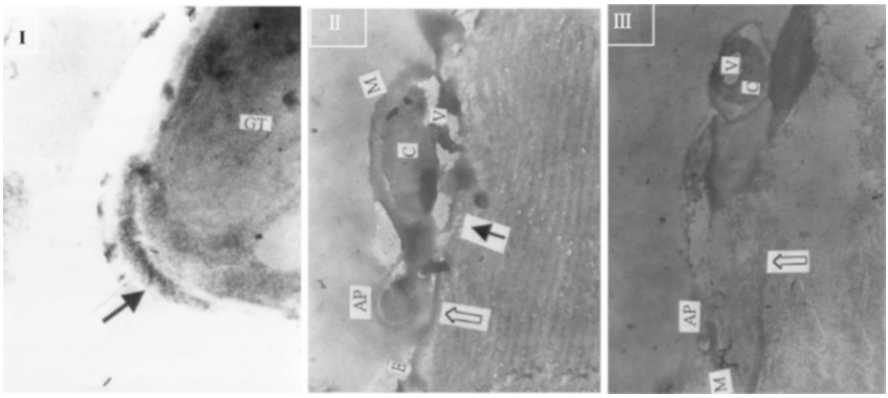

Fig. 11.11 Mucilage and appressorial structure under TEM (*I*) double mucilage cover on the tip of the germ tube (*arrow*), scale bar = 100 nm; (*II*) cross section of appressorium on epicuticle of *P. xylostella* infected by strain Bb-100, disappeared epicuticle part (*dark arrow*), scale bar = 500 nm; (*III*) appressorium on epicuticle of *P. xylostella* infected by strain Bb-62, disappeared epicuticle part (*arrow*), scale bar = 500 nm; conidia (C), germ tube (GT), appressorium (AP), vacuole (V), mucilage (M), epicuticle (E) (cf. Wang 1999; You et al. 2004)

A study of mummified larvae demonstrated that hyphae exit first at the abdomen region, but eventually appeared over the entire body (Wang 1999).

11.3.2 Enzyme Activities

11.3.2.1 Superficial Chitinase Profiles Under SEM

Bb-100 applied on the head of *P. xylostella* demonstrated an enzyme activity (arrow) (Figs. 11.8II and 11.9II on *P. xylostella*), as breaking down cuticle. Findings under SEM proposed that (1) releasing of chitinase on host depends on substrate contacted, being in agreement with reports (Coudron et al. 1984; St. Leger et al. 1996) and strain, and (2) some kinds of chitinases must be activated by proteinase before expressing activity because of their existing form of zymogen (Gooday et al. 1986). As consideration, there are some kind of substances that can induce the release of chitinase on elytra, and (3) chitinase is of potential in facilitating invasion, regardless of strain's pathogenicity.

11.3.2.2 Chitinase and Chitin Labeling Under TEM

According to the report, chitinases from different pathogens shared 66 % identity among them (St. Leger et al. 1996). For this reason, an antibody-ConA complex was applied to detect chitinase activity during invasion. Unfortunately, poor results

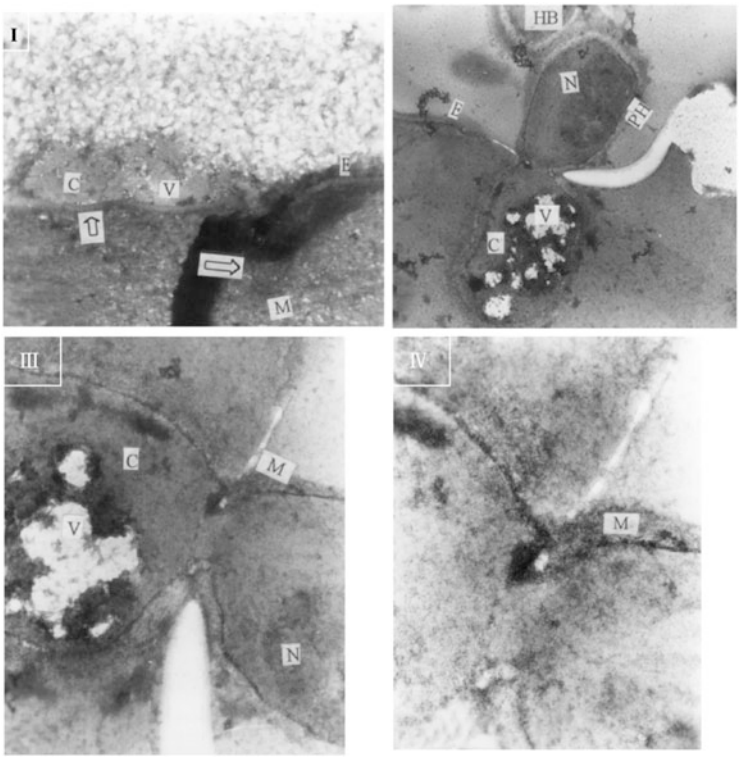

Fig. 11.12 Invasion of the cuticle of *P. xylostella* infected by Bb-100 under TEM (*I*) initial stage of invasion by the germ tube on the epicuticle after over 36 h, deformed epicuticle part due to mechanical pressure by the conidium (*arrow*), invading hyphae (*white arrow*), scale bar = 500 nm (*II–IV*) late stages of invasion of the cuticle after over 48 h, leakage of the cuticle (*arrow*), (*II*) scale bar = 200 nm, (*III*) scale bar = 200 nm, (*IV*) scale bar = 100 nm; conidia (C), appressorium (AP), vacuole (V), mucilage (M), epicuticle (E), nuclei (N), hyphal body (HB), penetrating hyphae (PH), lamellate structure (LS) (cf. Wang 1999; You et al. 2004)

were obtained. Another method was tried instead of primer with good results. Results under TEM indicated that chitinase activity could be detected through infection stage on the second instar cuticle of both *P. xylostella*, but was rare to see in later stages after penetration. Figure 11.14I–III provides a superficial show of chitinase activity before breaching *P. xylostella*. Before germination (24 h), gold particles are almost only distributed near conidia, and only a few particles were observed in conidia (Fig. 11.14III). This probably gives evidence concerning the level of chitinase activity. When germination occurred (over 36 h), large amounts of gold particles were found within the outer layer and near the germ tube. However, a few gold particles were found on the germ tube surface (Fig. 11.14II). In later penetration stage, chitinase was not labeled because hyphae had penetrated into the cuticle fully at this stage, and very little chitinase was required. Therefore,

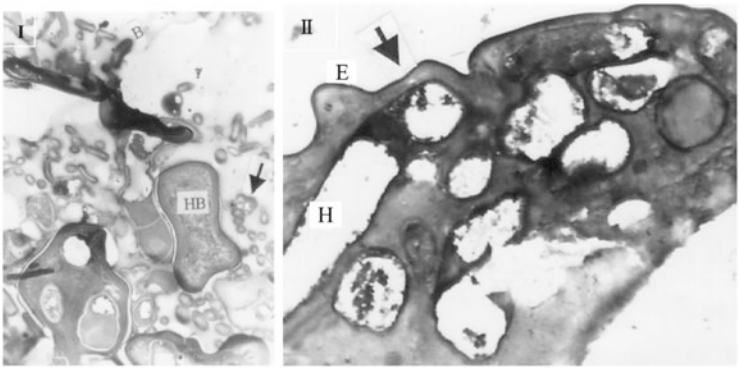

Fig. 11.13 (*I*) Rapid growth of hyphae inside the host after over 6 days under TEM, hemocyte (*arrow*), scale bar = 2 μm, (*II*) detailed view of the destroyed cuticle of *P. xylostella* after over 6 days under TEM, destroyed cuticle (*arrow*), scale bar = 1 μm; hyphae body (HB), hyphae (H), blastospore (B), epicuticle (E) (cf. Wang 1999; You et al. 2004)

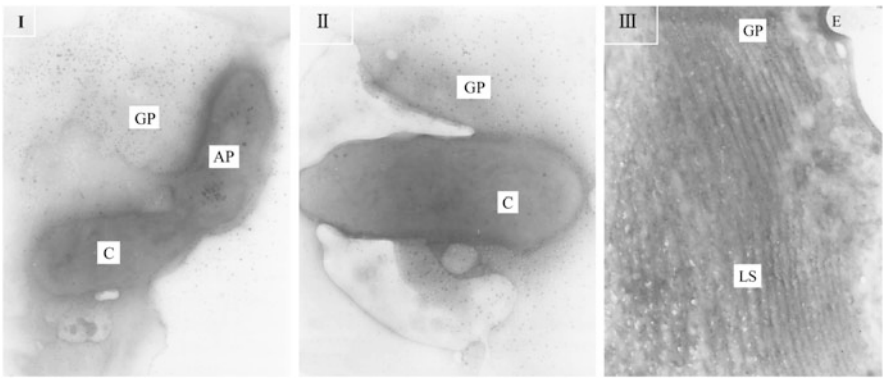

Fig. 11.14 Germinated conidia under the epicuticle of *P. xylostella* under TEM (*I*) infected by strain Bb-100, 10 nm gold particles mainly distributed around conidia, a lot of particles on the surface of appressoria (*II*) infected by strain Bb-62, 10 nm gold particles mainly distributed around conidia, a lot of particles on the wall of conidia (*III*) detailed view of the cross section of the labeled cuticle of *P. xylostella*, 30 nm gold particles distributed at random on the cuticle; conidia (C), appressoria (AP), gold particle (GP), epicuticle (E), lamellate structure (LS); scale bar = 200 nm (cf. Wang 1999; You et al. 2004)

it is hard to detect the lowest enzyme activity within conidia and germ tubes (Fig. 11.12II with strain Bb-100 on *P. xylostella*).

Chitin is an unbranched polysaccharide, composed primarily of β-1,4-linked *N*-acetylglucosamine (NAG) residue, with an occasional glucosamine residue (Brimacomge and Webber 1964). The best documented pathway for the degradation of chitin involves the sequential action of two separate hydrolases: (1) endochitinase [poly-β-1,4-(2 acetamido-2-deoxy)-D-glucoside glycanhydrolase (EC-3.2.1.14)], which produces low-molecular-weight soluble multimers of NAG,

the titer from *N*,*N*-diacetyl chitobiose being predominant, and (2) chitobiase or exochitinase [chitobiase acetylaminodeoxyglucohydrolase (EC 3.2.1.29)], which hydrolyses the intermediates to NAG (Coudron et al. 1984). Conidia, both Bb-100 and Bb-62 germinated to form germ tubes on the surface of the third instar of *P. xylostella* and penetrated cuticles within 40 h. The thin section of the cuticle at 16, 24, 36, 48, and 60 h post-inoculation was labeled with antibody to chitinase and gold-polysaccharide complexes (dehydroxy chitin), respectively. In spite of their 66 % identity in sequence, there were still sequence differences between chitinase in *B. bassiana* and *Serratia marcescens*, whereas in experiments, just a few gold particle were found around conidia (Wang 1999). The failure to detect chitinase via antibody probably is a good explanation to this menace. Firstly, gold-polysaccharide complexes were used to show distribution of chitinase; no such thing has been reported before. The polysaccharide applied contains a variety of collection including titer of NAG, multimer of NAG, and glycol chitin, which can be taken as substrate by whatever endochitinase to degrade into NAG. Therefore, it is possible to label endochitinase in fungi by using such complexes. In addition, gold-chitinase was employed to examine chitin distribution both in fungi (Bb100, Bb62) and cuticle, but only later was labeled on *P. xylostella* (Fig. 11.14III). The failure to label chitin in hypha hints that it is just an evaluated protecting strategy for fear that fungi would be destroyed by chitinase released by themselves.

11.4 Metabolites

Numerous factors (slow action, potentially negative interactions with commonly used fungicides, limited shelf life, and dependence on favorable environmental conditions) continue to impede the commercial development and/or application of this fungus (Wang et al. 2007). *B. bassiana* requires high humidity for germination, for establishment of infection, and for sporulation and consequent epizootics, which commonly facilitates epizootics of plant disease. These factors became bottlenecks in the application of *B. bassiana* in DBM control. *B. bassiana* produces secondary metabolites with insecticidal properties during the colonization of the host tissue, which may play an important role in host mortality. Recently, the toxic substances extracted from *B. bassiana* have been found to be potent against DBM in the laboratory and at field levels. Gao et al. (2012) found that the fermentation filtrate of strain Bb-2 had bioactive and virulent properties against the larvae of *P. xylostella* with the corrected mortality of 26.7 % and 35.6 % 24 h and 48 h after treatment with fermentation filtrate.

11.5 Conclusion and Future Prospects

Future studies should be directed toward the definition of recognition factors which are involved in (1) the attachment; (2) chemical recognition between the emerging hyphal tip of germination conidia and surface of epicuticle, resulting in the hyphal tip taxis toward cuticle and penetration; (3) enzyme activity; and (4) appressoria formation. In conclusion, the application of toxic secondary metabolites from *B. bassiana* has broken through the bottlenecks in the application of *B. bassiana* for the control of diamondback moth.

References

Bidochka MJ, Miranpuri GS, Khachatourians GG (1993) Pathogenicity of *Beauveria bassiana* (Balsamo) Vuillemin toward lygus bug (Hem., Miridae). J Appl Entomol 115:313–317

Brimacomge JS, Webber JM (1964) Mucopolysaccharides: chemical structure, distribution and isolation. Elsevier, Amsterdam, pp 18–42

Butt TM, Jackson C, Magan C (2001) Fungi as biocontrol agents: progress, problems and potential. CABI Publishing, UK

Coudron TA, Kroha MJ, Ignoffo CM (1984) Levels of chitinolytic activity during development of tree entomopathogenic fungi. Comp Biochem Physiol 79B:339–348

Fan M, Li Z (1994) Impact of nutrients and culture conditions on appressorium formation of entomogenous fungi. J Aanhui Agric Univ 21:123–130

Gao P, Hu Q, Wang Y (2012) Virulence of spores and fermentation filtrates of *Beauveria bassiana* Bb-2. Hubei Agric Sci 51:3237–3239

Gooday GW, Humphreyas M, Mcintoshw H (1986) Roles of chitinases in fungal growth. In: Muzzarelli CJ, Gooday GW (eds) Chitin in nature and technology. Plenum, New York, pp 83–91

Lacey LA, Goettel M (1995) Current development in microbial control of insect pests and prospects for the early 21st century. Entomophaga 40:3–27

Large JP, Monsigny M, Prevost MC (1988) Visualization of exocellular lectins in the entomopathogenic fungus *Conidiobolus obscurus*. J Histochem Cytochem 36:1419–1424

Masuda T (1998) Microbial control of diamond back moth, *Plutella xylostella*, by entomopathogenic fungus, *Beauveria bassiana*. In: Meeting Program and Abstracts VII Inter. Coll. Invertebr. Path. & Microb. Contr. IVth Inter. Confer. on *Bacillus thuringiensis*, Sapporo, 23–28 August 1998

St. Leger RJ, Butt TM, Mark S et al (1989) Production in vitro of appressoria by the entomopathogenic fungus *Metarhizium anisopliae*. Exp Mycol 13:274–288

St. Leger RJ, Roberts DW, Staples RC (1991) A model to explain differentiation of appressoria by germlings of *Metarhizium anisopliae*. J Invertebr Pathol 57:299–310

St. Leger RJ, Bidochka MJ, Donald WR (1994) Germination triggers of *Metarhizium anisopliae* conidia are related to host species. Microbial 140:1651–1660

St. Leger RJ, Joshi L, Gidochka MJ, Nancy W et al (1996) Characterization and ultrastructure localization of chitinases from *Metarhizium anisopliae*, *M. flavoviride*, and *Beauveria bassiana* during fungal invasion of host (*Manduca sexta*) cuticle. Appl Environ Microb 62(3):907–912

Wang H (1999) Ultrastructural studies on infection behaviors of *Beauveria bassiana* to *Plutella xylostella*. Ph.D. Thesis, Fujian Agricultural University, Fuzhou

Wang L, Huang J, You M, Guan X, Liu B (2007) Toxicity and feeding deterrence of crude toxin extracts of *Lecanicillium (Verticillium) lecanii* (Hyphomycetes) against sweet potato whitefly (*Bemisia tabaci*; Hom., *Aleyrodidae*). Pest Manag Sci 63:381–387

Wang L, You M, Huang J, Zhou R (2010) Diversity of entomopathogenic fungi and their application on biological control. Acta Agric Univ Jiangxiensis 32:920–927

You M, Hou Y, Yang G (2004) Control of the population system of Diamond back moth *Plutella xylostella*. Fujian Science and Technological Press, Fuzhou

Zhai J, Huang X (1995) Review on pathogenicity mechanism of entomopathogenic fungi, *Beauveria bassiana*. Mycology 22:45–48

Zhai J, Huang X (1997) Studies on behavior of germination of conidia from *Beauveria bassiana* on the cuticle of *Heliothis zea*. Acta Microbiol Sin 37:154–158